

Low-Field Magnetization Reversal in Fe/Ag Granular Films

Hiroshi Sakuma, Yuki Saito*, Hiroki Hamakake**, Takayuki Kashiwakura, and Kiyoshi Ishii

Department of Electrical and Electronic Engineering, Utsunomiya University, 7-1-2 Yoto, Utsunomiya 321-8585

Fax: 81-28-689-6090, e-mail: hsakuma@cc.utsunomiya-u.ac.jp

Fe/Ag films were prepared by a gas flow sputtering technique. The granular structure in which Fe nanoparticles were embedded in an Ag matrix was confirmed by transmission electron microscopy, x-ray diffraction, and x-ray photoelectron spectroscopy. The magnetic property depended on the Fe/Ag relative composition: A film with Fe content of less than 30at% was superparamagnetic and a film with higher Fe content was ferromagnetic at room temperature. The coercivity of the ferromagnetic films increased with the increase in Fe content. Fe/Ag films with Fe contents of 30 to 40at% showed a low coercivity (a few hundred amperes per meter) and a high squareness (above 0.5). The low-field magnetization reversal was attributable to interparticle magnetic interaction.

Key words: Fe/Ag, granular film, magnetization reversal, interparticle interaction

1. INTRODUCTION

Spin electronic devices make use of electrical conduction which depends on the direction of magnetization. In magnetic devices such as magnetic random access memory, it is desired that the field strength required for the magnetization reversal is small. Low-field magnetization reversal of such a magnetic element is achieved by lowering the energy barrier of domain wall motion. However, for device miniaturization, the magnetic element is becoming smaller and approaching the scale of a single magnetic domain. In addition, a single domain particle may be used for a future device using spin-selective single-electron transfer [1]. Thus, interest has been shown in low-field magnetization reversal of a single domain particle.

It is well known that the initial susceptibility of a single domain particle is maximum at blocking temperature. This means that low-field magnetization reversal is achieved at the blocking temperature, but the magnetization is usually small at that temperature. It has

been also known for over twenty years that particles with magnetic interaction exhibit a cooperative magnetic-ordering phenomenon and that the initial susceptibility is greatest at the ordering temperature [2]. However, a little attention has been paid to the magnetization reversal field of an interacting particle system.

In this study, we prepared magnetic nanoparticles embedded in a nonmagnetic matrix and observed a low-field magnetization reversal. Its origin is discussed in terms of the interparticle interaction.

2. EXPERIMENT

Samples used in this study were Fe/Ag films prepared by co-deposition of Fe clusters and Ag atoms using a gas flow sputtering technique [3]. Tubes of Fe and Ag were used as sputtering targets. The internal diameters of the targets and the distance between target and substrate were optimized for the deposition of Fe in the form of particles and Ag in the form of a film. The composition was measured by using inductively coupled plasma

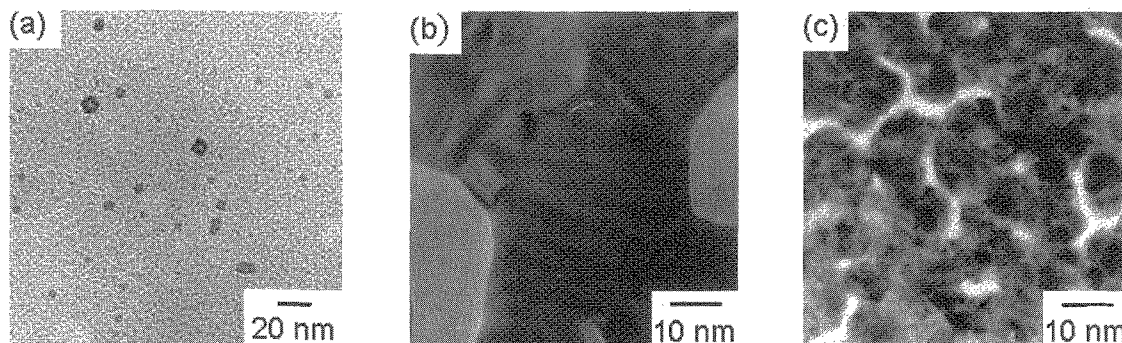


Fig. 1 TEM images of (a) Fe, (b) Ag, and (c) Fe18at%/Ag deposit on TEM grids.

* Present affiliation: Canon Electronics Inc.

** Present affiliation: Hitachi Metals, Ltd.

spectroscopy. Magnetization curves were obtained by using a vibrating sample magnetometer with a maximum field of 1.6 MA/m. X-ray photoelectron spectroscopy was performed after ion etching to remove the surface and prove the interior of the film.

3. RESULTS AND DISCUSSION

3.1 Structure

Figures 1 (a) to (c) show transmission electron microscope (TEM) images of Fe, Ag, and Fe/Ag deposits on TEM grids. Fe is in the form of particles that have a diameter of about 5 nm, while Ag is in the form of a film. For an Fe/Ag film, Fe particles are embedded in an Ag matrix.

As shown in Fig. 2, the x-ray diffraction peak of Fe is broad, while that of Ag is sharp. This indicates that the crystallite is larger for Ag and smaller for Fe, agreeing with the TEM images. Since the peak positions of Fe 110 and Ag 200 are close to each other, the peak at about 45° of the Fe/Ag film cannot be identified. Figure 3 shows the spacing of the Ag {111} plane estimated using the peak position as a function of composition. The line denotes the spacing based on the assumption of Vegard's law with fcc Ag [4] and fcc γ -Fe [5]. The maximum change in the Ag {111} spacing corresponds to a solid solution in which a small percentage of Ag atoms are substituted by Fe atoms based on Vegard's law, whereas the solubility of Fe and Ag is very low in an equilibrium state [6]. This nonequilibrium state of high solubility is likely to be attributed to the mixing of low-energy Fe clusters and Ag atoms. A similar change in lattice spacing was observed for an Fe/Ag film prepared by a sputter-gas aggregation technique [7]. It should be noted that most of the Fe atoms are not substituted with Ag but form Fe particles.

Figure 4 shows x-ray photoelectron spectra of Fe36at%/Ag and Fe70at%/Ag films. The Fe70at%/Ag film obviously contains oxidized Fe atoms, while the Fe36at%/Ag film has less oxidized Fe atoms and most of the Fe atoms are metallic. A quantitative analysis of the spectra reveals that the Fe36at%/Ag and Fe70at%/Ag films contain 6at% and 25at% oxygen, respectively. Oxidized Ag atoms are not detected in these films.

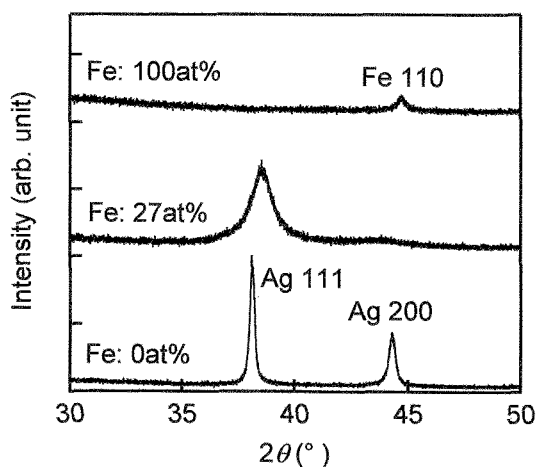


Fig. 2. XRD patterns of Fe, Fe27at%/Ag, and Ag deposits on glass substrates. Cu K α radiation was used.

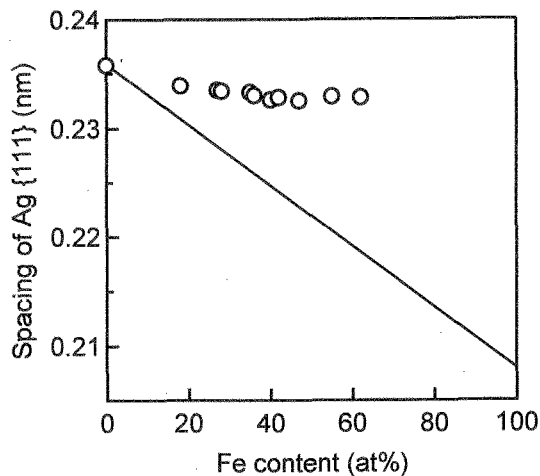


Fig. 3. Relationship between spacing of the Ag {111} plane and Fe content.

The above results indicate that the Fe/Ag deposit has a granular structure in which Fe nanoparticles are embedded in an Ag matrix. Most of the Fe atoms in the film with a low Fe content are not oxidized but are in a

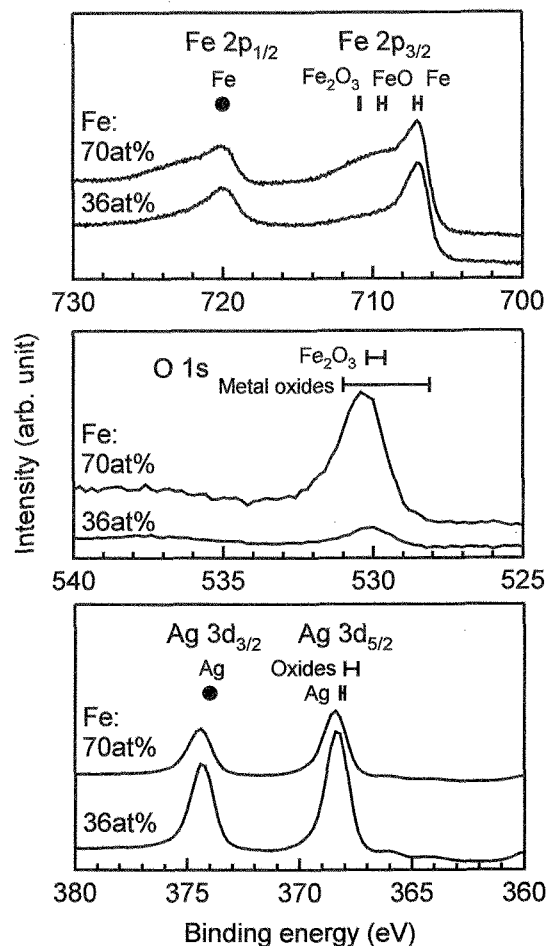


Fig. 4. XPS spectra of Fe36at%/Ag and Fe70at%/Ag films. Reference values of binding energy for some oxidation states [8] are also shown.

metallic state.

3.2 Magnetic properties

Figure 5 shows magnetization curves as a function of composition. The Fe/Ag film with a low Fe content is superparamagnetic, and it becomes ferromagnetic as Fe content increases. At an Fe content of 30 to 40at%, the Fe/Ag film is soft magnetic: the field strength required to reverse magnetization is very small. As shown in Fig. 6, coercivity is close to zero at Fe content below 30at%, and it increases with increase in Fe content in the region of Fe content of 30 to 60at%. The squareness defined as remanence divided by saturation magnetization takes a maximum of 0.77 at Fe34at%. At Fe content of 30 to 40at%, coercivity is low and squareness is high, which means that the magnetization is easily aligned parallel to the applied field.

Figure 7 shows the temperature dependence of zero-field-cooled magnetization normalized by field-cooled magnetization at 5 K (M_{ZFC}/M_{FC} at 5K). A field of 8 kA/m was applied for the measurement of magnetization. The parameter M_{ZFC}/M_{FC} at 5K is interpreted as a measure of magnetic softness and closely analogous

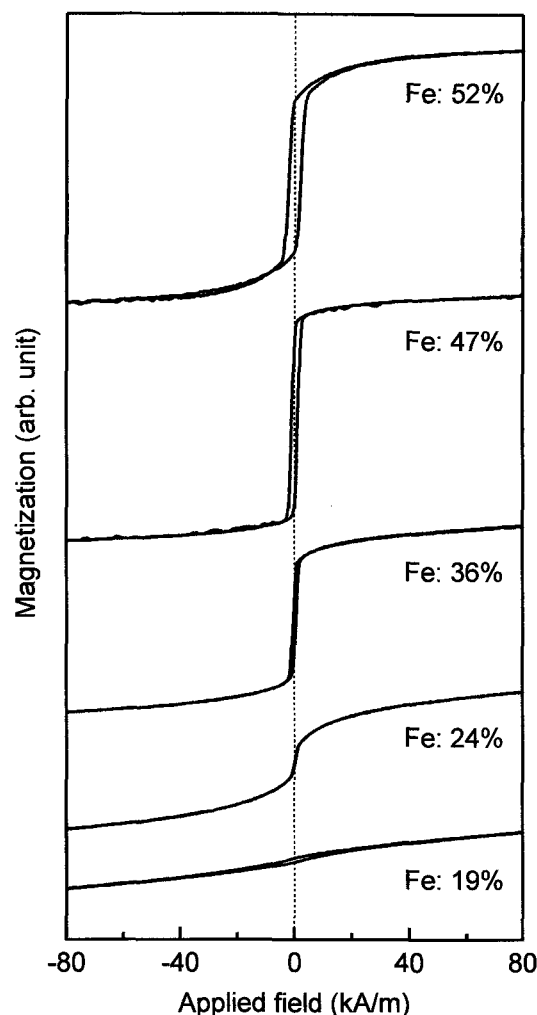


Fig. 5. In-plane magnetization curves at room temperature as a function of composition.

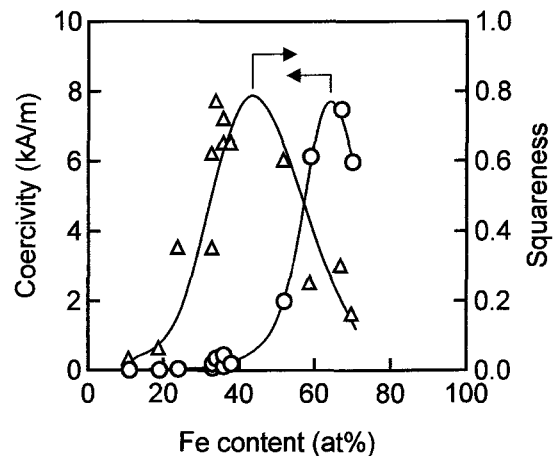


Fig. 6. Coercivity and squareness as a function of composition. The squareness is defined as remanence divided by saturation magnetization.

to initial susceptibility χ_i . The temperature at which M_{ZFC}/M_{FC} at 5K shows a maximum value increases and approaches room temperature with increasing Fe content. It is noted that the applied field of 8 kA/m is rather high, and it shifts the peak to lower temperature.

The peak of χ_i can be seen in a magnetically isolated fine particle at its blocking temperature T_B . Wohlfarth [9] derived a theoretical relationship between χ_i and temperature T for a fine particle system without interaction:

$$\chi_i = M_s^2 v / 3k_B T, \quad (1)$$

where M_s is saturation magnetization, v is volume of a particle, and k_B is the Boltzmann constant. This Curie law-type equation is applicable only to temperatures above T_B , and the maximum value of χ_i , which is achieved at T_B , is a finite value. T_B increases with the increase in particle size.

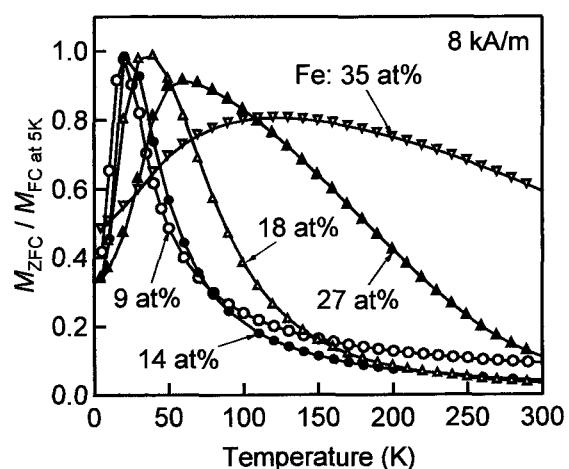


Fig. 7 Zero-field-cooled magnetization normalized by field-cooled magnetization at 5 K. A field of 8 kA/m was applied for the measurement of magnetization.

On the other hand, the relationship between χ_i and T of a fine particle system with interaction was derived by El-Hilo et al. [10]. If particle size distribution is omitted, χ_i is described as follows:

$$\chi_i = M_s^2 v / 3k_B(T - T_0), \quad (2)$$

where T_0 is ordering temperature which reflects the strength of interparticle interaction. This Curie-Weiss law-type equation means that χ_i is infinite at $T = T_0$. Therefore, if T_0 is equal to room temperature, infinite χ_i is expected at room temperature. The difference between the particle systems with and without interaction is illustrated in Fig. 8.

The fine particle systems with and without interaction both show a peak of χ_i at T_B or T_0 . The shift of peak in Fe/Ag films is attributed to the change in the strength of the interaction. We previously reported that T_0 of a Fe/Ag film is close to zero at a low Fe content and increases with increase in Fe content. [11] T_0 of an Fe27at%/Ag film is 220 K, and Fe/Ag films with Fe content of 30 to 40at% are likely to have higher T_0 . The high ordering temperature originating in the interparticle interaction is the most likely origin of the low-field magnetization reversal in Fe/Ag films.

The mechanism of interparticle interaction is important for understanding the magnetic-ordering phenomenon of particle system. Although we have not obtained enough results, ΔM plot [12] of a Fe35at%/Ag film indicates that the interparticle interaction is a strong one such as exchange interaction.

4. SUMMARY

We prepared Fe/Ag granular films in which Fe nanoparticles were embedded in an Ag matrix by gas flow sputtering. Fe/Ag films with Fe content of 30 to 40at% showed low coercivity of a few hundred amperes per meter and a high squareness above 0.5. This low-field magnetization reversal was attributed to interparticle magnetic interaction.

References

- [1] K. Majumdar and S. Hershfield, *Phys. Rev. B*, **57**, 11521-11526 (1998).
 [2] K. O'Grady, A. Bradbury, S. W. Charles, S. Menear,

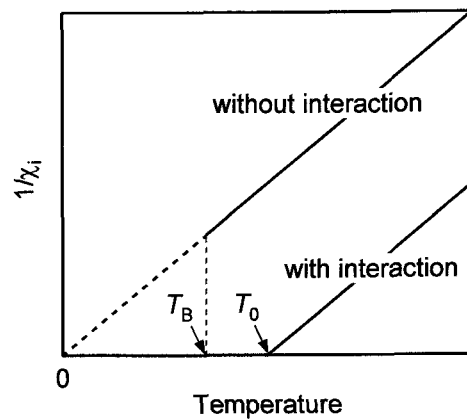


Fig. 8. Theoretical relationship between reciprocal of initial susceptibility χ_i and temperature for fine particle systems with and without magnetic interaction. T_0 and T_B are ordering temperature and blocking temperature, respectively.

- and J. Popplewell, *J. Magn. Magn. Mater.*, **31-34**, 958-960 (1983).
 [3] H. Hamakake and K. Ishii, *IEEE. Trans. Magn.*, **33**, 3457-3459 (1999).
 [4] JCPDS powder diffraction file, 4-783.
 [5] JCPDS powder diffraction file, 31-619.
 [6] "Alloy Phase Diagrams", Ed. by H. Baker, ASM international, Materials Park (1992) pp. 2.29.
 [7] G.-F. Hohl, T. Hihara, M. Sakurai, T. J. Konno, K. Sumiyama, F. Hensel, and K. Suzuki, *Appl. Phys. Lett.*, **66**, 385-387 (1995).
 [8] J. F. Moulder, W. F. Stickle, P. E. Sobol, and K. D. Bomben, "Handbook of X-ray Photoelectron Spectroscopy", Physical Electronics, Eden Prairie (1995).
 [9] E. P. Wohlfarth, *Phys. Lett.*, **70A**, 489-491 (1979).
 [10] M. El-Hilo, K. O'Grady, and R. W. Chantrell, *J. Magn. Magn. Mater.*, **117**, 21-28 (1992).
 [11] H. Hamakake, M. Wakairo, M. Ishikawa, and K. Ishii, *IEEE. Trans. Magn.*, **36**, 2875-2878 (2000).
 [12] K. O'Grady, R. W. Chantrell, and I. L. Sanders, *IEEE Trans. Magn.*, **29**, 286-291 (1993).

(Received January 11, 2005) ; Accepted March 11, 2005)